

A new complementary mild-slope equation

By JANG WHAN KIM¹ AND KWANG JUNE BAI²

¹Department of Ocean and Resources Engineering, SOEST, University of Hawaii at Manoa
and American Bureau of Shipping, 16855 Northchase Drive, Houston, TX77060, USA

²RIMSE and Department of Naval Architecture and Ocean Engineering,
Seoul National University, Korea

(Received 15 March 2001 and in revised form 25 September 2003)

A new depth-integrated equation is derived to model a time-harmonic motion of small-amplitude waves in water of variable depth. The new equation, which is referred to as the complementary mild-slope equation here, is derived from Hamilton's principle in terms of stream function. In the formulation, the continuity equation is satisfied exactly in the fluid domain. Also satisfied exactly are the kinematic boundary conditions at the still water level and the uneven sea bottom. The numerical results of the present model are compared to the exact linear theory and the existing mild-slope equations that have been derived from the velocity-potential formulation. The computed results give better agreement with those of the exact linear theory than the other mild-slope equations. Comparison shows that the new equation provides accurate results for a bottom slope up to 1.

1. Introduction

The mild-slope equation has been widely used as an approximate model for the refraction and diffraction of the linear surface waves in water of variable depth after the pioneering work of Berkhoff (1973). In this model, a vertical-averaging procedure is introduced to reduce the governing equations of the full three-dimensional theory to the depth-integrated equations in the horizontal plane. The assumption of mild slope is made in order to ignore the higher-order terms that contain bottom slope and curvature from the depth-integrated equations. The mild-slope equation is known to work very well for a bottom slope of less than 1/3 (see Booij 1983). Recently, many attempts have been made to improve the existing mild-slope equations. To name a few, Massel (1993) and Chamberlain & Porter (1995) derived the modified mild-slope equation using variational principles and keeping the higher-order terms that were neglected in Berkhoff's original derivation. Kirby (1986) used a similar approach to consider the slope of the rapidly varying component of a ripple bed. Porter & Staziker (1995) further extended the model by introducing eigenfunctions for the evanescent modes in addition to the propagating mode. They also provided the correct jump condition for the modified mild-slope equation in the presence of a bottom slope discontinuity, which was not properly given in Chamberlain & Porter (1995). However, Athanassoulis & Belibassakis (1999) pointed out that the eigenmodes used in the derivation of the modified mild-slope equations could not satisfy the boundary condition at the uneven sea bottom. As a remedy, they added an additional term to satisfy the condition and improved the convergence of the solution to the exact linear theory. In a similar line of approach, Chandrasekera & Cheung (2001) proposed a two-term expansion of the velocity profile, which satisfies

the kinematic boundary conditions on the sea bottom exactly. A more thorough literature survey can be found in Athanassoulis & Belibassakis (1999).

In the present study, we propose an alternative approach to satisfy the bottom boundary condition exactly. Instead of the potential formulation that has been used in the previous models, we introduce a variational principle in terms of the streamfunction theory, which is also known as the complementary variational principle (see e.g. Bai 1977). It should be noted that the definition of the streamfunction is extended to the two-component vector potential in a three-dimensional fluid domain (see Kim *et al.* 2001). In this streamfunction formulation, the continuity equation in the fluid domain is also satisfied, as well as the boundary condition on the sea floor. The variational principle is stated as the stationary condition of a time-averaged Lagrangian, as described in §2.1. The new mild-slope equation is derived from the solution of the variational problem after restricting the vertical profile of the trial solution as that of the progressive wave solution in the uniform depth in §2.2. We refer to the new equation as the complementary mild-slope equation. In §3.1, a term-by-term comparison with the existing mild-slope equations is made after the complementary mild-slope equation is expanded with respect to bottom slope and curvature. When the second-order terms, such as the bottom curvature and quadratic of the bottom slope, were neglected, the complementary mild-slope equation reduced to Berkhoff's original mild-slope equation. However, the second-order terms of the complementary mild-slope equation did not agree with those of the modified mild-slope equation.

The new complementary mild-slope equation is applied to the wave diffraction over one-dimensional bathymetry. The jump condition over the discontinuity of the bottom slope and the radiation condition are derived in §4.1. As a numerical implementation, the finite-element method is applied after the weak formulation of the complementary mild-slope equation, as described in §4.2.

A systematic computation is made to test the accuracy of the complementary mild-slope equation and results are compared with those of previous mild-slope equations based on velocity-potential formulation in §5. The new model provides better prediction of the wave diffraction over the ripple bed and bottom mound than the mild-slope equation and the modified mild slope equation.

2. Mathematical formulation

The motion of an inviscid and incompressible fluid with a free surface has usually been formulated in terms of the velocity potential, which is governed by the Laplace equation in the fluid domain with appropriate boundary conditions. The exact free-surface-wave problem is a free-boundary problem which is difficult to solve. To remedy this difficulty, it is customary to linearize the nonlinear free-surface boundary condition and we obtain a well-posed boundary-value problem in the potential theory. This boundary-value problem can also be formulated by classical variational principles used in the previous derivation of the mild-slope equation (e.g. Chamberlain & Porter 1995; Miles & Chamberlain 1999). We make use of Hamilton's principle to derive a complementary mild-slope equation. In the principle, the solution can be obtained as the stationary point of a time-averaged Lagrangian among the divergence-free velocity fields that satisfy the kinematic boundary conditions exactly. The Hamilton principle used here is different from that used in the derivations of the potential-based mild-slope equations (see, for example, Miles & Chamberlain 1999). In the present approach, the continuity equation and the kinematic boundary conditions are treated

as the kinematic constraints and are satisfied exactly, while the irrotational condition in the fluid domain and the dynamic boundary condition on the mean water level are satisfied on average (i.e. in a weak sense). On the other hand, in the variational principle in potential formulation, the irrotational condition is treated as a constraint and satisfied exactly while the continuity equation is satisfied in a weak sense. The details on Hamilton's principle and the derivation of the complementary mild-slope equation are given in the next section.

2.1. The variational principle

We consider the linear wave motion over a variable bottom topography, $z = -h(x, y)$. The Cartesian coordinate system $Oxyz$ is defined such that the vertical coordinate z directs upward and the Oxy -plane is the still-water plane. We introduce complex-valued functions $\zeta(x, y)$, $\mathbf{u}(x, y, z)$ and $w(x, y, z)$ to define the time-harmonic motion of the wave elevation, horizontal velocity vector and vertical velocity component as, $\text{Re}[\zeta e^{-i\omega t}]$, $\text{Re}[\mathbf{u} e^{-i\omega t}]$ and $\text{Re}[w e^{-i\omega t}]$, respectively, where ω is the circular frequency of the incoming wave.

The time-averaged Lagrangian for this problem is given by

$$\left. \begin{aligned} \bar{L} &= \iint L \, dx \, dy, \\ L &= \frac{1}{2}\rho \int_{-h(x,y)}^0 \{|\mathbf{u} \cdot \mathbf{u}|^2 + |w|^2\} \, dz - \frac{1}{2}\rho g |\zeta|^2, \end{aligned} \right\} \quad (1)$$

where ρ and g are the density of the fluid and gravitational constant, respectively, and L denotes the Lagrangian density. Hamilton's principle states that the true solution of the equation of motion makes the time-averaged Lagrangian have a stationary value among the trial solutions that satisfy the kinematic constraints. The kinematic constraints in this problem consist of the continuity equation in the fluid domain and the kinematic boundary conditions on the bottom and the free surface:

$$\nabla \cdot \mathbf{u} + \frac{\partial w}{\partial z} = 0, \quad -h < z < 0, \quad (2)$$

$$w + \nabla h \cdot \mathbf{u} = 0, \quad z = -h, \quad (3)$$

$$i\omega\zeta + w = 0, \quad z = 0, \quad (4)$$

where $\nabla = (\partial/\partial x, \partial/\partial y)$.

Equations (2), (3) and (4) can be satisfied by introducing a vector potential

$$\Psi(x, y, z) \equiv \int_{-h}^z \mathbf{u}(x, y, z_0) \, dz_0, \quad (5)$$

from which the velocity field and wave elevation are defined as

$$\mathbf{u} = \frac{\partial \Psi}{\partial z}, \quad w = -\nabla \cdot \Psi, \quad (6)$$

$$\zeta = \frac{1}{i\omega} \nabla \cdot \Psi(x, y, 0). \quad (7)$$

Note that the bottom boundary condition, (3), is satisfied exactly, because $\Psi = 0$ at $z = -h$ by (5), which leads to $\nabla \cdot \Psi(x, y, -h(x, y)) = \nabla \cdot \Psi - \nabla h \cdot (\partial \Psi / \partial z) = -w - \nabla h \cdot \mathbf{u} = 0$. Substituting (6) and (7) into (1), the averaged Lagrangian density is

given by

$$L = \frac{1}{2}\rho \int_{-h(x,y)}^0 \left\{ |\nabla \cdot \Psi|^2 + \left| \frac{\partial \Psi}{\partial z} \right|^2 \right\} dz - \frac{\rho}{2\nu} |\nabla \cdot \Psi(x, y, 0)|^2, \quad (8)$$

where $\nu = \omega^2/g$. By setting the first variation to be zero, we obtain the following differential equation as a governing equation and boundary condition for $\Psi(x, y, z)$.

$$\nabla(\nabla \cdot \Psi) + \frac{\partial^2 \Psi}{\partial z^2} = 0, \quad -h < z < 0, \quad (9)$$

$$\frac{\partial \Psi}{\partial z} + \frac{1}{\nu} \nabla(\nabla \cdot \Psi) = 0, \quad z = 0. \quad (10)$$

In taking variations of (8), it was assumed that $\delta\Psi$ vanishes on some lateral boundaries, which implies that the normal velocity is specified on the lateral boundary.

It can be shown that (9) and (10) lead to irrotationality of the fluid velocity. The vorticity of the fluid motion can be given by

$$\left(\nabla + \mathbf{k} \frac{\partial}{\partial z} \right) \times \mathbf{u} = \mathbf{k} \times \left\{ \nabla(\nabla \cdot \Psi) + \frac{\partial^2 \Psi}{\partial z^2} \right\} + \nabla \times \frac{\partial \Psi}{\partial z}, \quad (11)$$

where \mathbf{k} is the unit vector in z -direction. The first term in the right-hand side of (11) vanishes because of (9). The vanishing of the second term can be shown after imposing $\nabla \times$ operator on (9) and (10).

In the two dimensions, where we can write $\Psi = (\psi, 0)$, (9) and (10) read

$$\frac{\partial^2 \psi}{\partial x^2} + \frac{\partial^2 \psi}{\partial z^2} = 0, \quad -h < z < 0, \quad (12)$$

$$\frac{\partial \psi}{\partial z} + \frac{1}{\nu} \frac{\partial^2 \psi}{\partial x^2} = 0, \quad z = 0, \quad (13)$$

which are the well-known Laplace equation and free-surface condition for stream-function (see e.g. Bai 1977).

2.2. The complementary mild-slope equation

In the case of uniform water depth, the boundary-value problem (12), (13) with $\psi(x, -h) = 0$ has a progressive wave solution,

$$\psi(x, z) = \sinh\{k(z+h)\} e^{ikx}, \quad (14)$$

where the wavenumber k is the real root of the following dispersion relation,

$$\nu = k \tanh kh. \quad (15)$$

Since a general analytical solution is not available in the case of variable water depth, we can seek for an approximate solution. To this end, we make use of the z -dependent behaviour (i.e. vertical mode) of the progressive wave solution in (14) and represent the solution in the following form:

$$\Psi(x, y, z) = \Psi_0(x, y) f(h, z), \quad f(h, z) = \frac{\sinh[k(h)(z+h)]}{\sinh k(h)h}, \quad (16)$$

where $k(h)$ is the local wavenumber defined in (15) and $\Psi_0(x, y)$ is the unknown function to be obtained. By substituting the assumed form of the solution given in (16) to (8), we obtain

$$L = \frac{1}{2}a |\nabla \cdot \Psi_0|^2 + \text{Re}\{b \nabla h \cdot \Psi_0 \nabla \cdot \Psi_0^*\} + \frac{1}{2}(-k^2 a + c \nabla h \cdot \nabla h) |\Psi_0|^2, \quad (17)$$

where $*$ denotes the complex conjugate and the coefficients a , b and c are real-valued functions of $h(x)$ and are defined by

$$a(h) = \int_{-h}^0 f^2 dz - \frac{1}{v} = -\frac{\coth kh}{2k} \left(1 + \frac{2kh}{\sinh 2kh} \right) = -\frac{gk^2}{\omega^4} CC_g, \quad (18a)$$

$$b(h) = \int_{-h}^0 f \frac{\partial f}{\partial h} dz = \frac{1}{4 \sinh^2 kh} \frac{2kh \cosh 2kh - \sinh 2kh}{2kh + \sinh 2kh}, \quad (18b)$$

$$c(h) = \int_{-h}^0 \left(\frac{\partial f}{\partial h} \right)^2 dz = \frac{k}{12 \sinh^2 kh} \frac{-12kh + 8k^3 h^3 + 3 \sinh 4kh + 12(kh)^2 \sinh 2kh}{(2kh + \sinh 2kh)^2}, \quad (18c)$$

where C and C_g are defined as the phase and group velocity of the plane progressive wave over a uniform depth h , which are given by

$$C \equiv \frac{\omega}{k} = \sqrt{g \tanh kh/k}, \quad C_g \equiv \frac{d\omega}{dk} = \frac{1}{2} C \left(1 + \frac{2kh}{\sinh 2kh} \right). \quad (19)$$

The Euler–Lagrange equation for the Lagrangian density given in (17) leads to the following complementary mild-slope equation:

$$-\nabla \{ a \nabla \cdot \Psi_0 + b \nabla h \cdot \Psi_0 \} + b \nabla h \nabla \cdot \Psi_0 + (-k^2 a + c \nabla h \cdot \nabla h) \Psi_0 = 0. \quad (20)$$

For a uniform depth, where $\nabla h = 0$ and $a = \text{const.}$, (20) reduces to

$$\nabla \{ \nabla \cdot \Psi_0 \} + k^2 \Psi_0 = 0. \quad (21)$$

Taking curl of (21), it can be shown that Ψ_0 is irrotational and can be written as $\Psi_0 = \nabla \Phi_0$, where the auxiliary scalar potential $\Phi_0(x, y)$ is a solution of the Helmholtz equation,

$$\nabla^2 \Phi_0 + k^2 \Phi_0 = 0. \quad (22)$$

Besides the uniform-depth case, the complementary mild-slope equation is in vector form as in (20), which is a disadvantageous property compared to the potential-based mild slope equations. In two-dimensional problems, however, the equation reduces to a single scalar equation. We consider the characteristics of the two-dimensional equation in the next section.

3. The complementary mild-slope equations in two dimensions

In two dimensions, where we can set $\Psi(x, y, z) = (\psi(x, z), 0)$ and $\Psi_0(x, y) = (\psi_0(x), 0)$, the complementary mild-slope equation, (20), can be written as

$$-\frac{d}{dx} \left(a \frac{d\psi_0}{dx} + bh' \psi_0 \right) + bh' \frac{d\psi_0}{dx} + (-k^2 a + h'^2 c) \psi_0 = 0, \quad (23)$$

where $h' \equiv dh/dx$.

In the next section, we compare the complementary mild-slope equation, (23), with the existing mild-slope equations based on the velocity potential formulation, such as the modified mild-slope equation and Berkhoff's original mild-slope equation.

3.1. Comparisons with modified mild-slope equations

When the bathymetry $h(x)$ is smooth, (23) can be written as

$$\frac{d}{dx} \left(a \frac{d\psi_0}{dx} \right) + \{ k^2 a + bh'' + (b_h - c)h'^2 \} \psi_0 = 0, \quad (24)$$

where $h'' \equiv d^2h/dx^2$ and $b_h \equiv db/dh$. Then, we will compare (24) with the modified mild-slope equation,

$$\frac{d}{dx} \left(u_0 \frac{d\phi}{dx} \right) + (k^2 u_0 + u_1 h'' + u_2 h'^2) \phi = 0, \quad (25)$$

and Birhoff's mild-slope equation,

$$\frac{d}{dx} \left(u_0 \frac{d\phi}{dx} \right) + k^2 u_0 \phi = 0, \quad (26)$$

where ϕ is the velocity potential on the still-water level and the coefficients are defined by

$$u_0(h) = \frac{\tanh kh}{2k} \left(1 + \frac{2kh}{\sinh 2kh} \right) = \frac{1}{g} C C_g, \quad (27a)$$

$$u_1(h) = \frac{1}{4 \cosh^2 kh} \frac{\sinh 2kh - 2kh \cosh 2kh}{2kh + \sinh 2kh}, \quad (27b)$$

$$u_2(h) = \frac{k \sec h^2 kh}{12(2kh + \sinh 2kh)^3} \{16(kh)^4 + 32(kh)^3 \sinh 2kh - 9 \sinh 2kh \sinh 4kh + 6kh(2kh + 2 \sinh 2kh)(\cosh^2 2kh - 2 \cosh 2kh + 3)\}. \quad (27c)$$

It should be noted that (26) can also be obtained from (25) after discarding the second-order terms, $h''(x)$ and $h'^2(x)$.

Although (24) and (25) are in the same structure, a direct comparison is not easy because the complementary mild-slope equation is given in terms of the streamfunction whereas the modified mild-slope equation is in terms of the velocity potential. In the following, we compare the two equations with each other after transforming both equations into the terms of the surface elevation ζ .

First, the transformation of the modified mild-slope equation can be made easily by the use of the relation $\zeta = i\omega\phi$:

$$\frac{d}{dx} \left(u_0 \frac{d\zeta}{dx} \right) + (k^2 u_0 + u_1 h'' + u_2 h'^2) \zeta = 0. \quad (28)$$

Further expansion of the first term gives

$$\frac{d^2 \zeta}{dx^2} + P_1 h' \frac{d\zeta}{dx} + (k^2 + P_2 h'' + P_3 h'^2) \zeta = 0, \quad (29)$$

where

$$P_1(h) = \frac{1}{u_0} \frac{du_0}{dh}, \quad P_2(h) = \frac{u_1}{u_0}, \quad P_3(h) = \frac{u_2}{u_0}. \quad (30)$$

Note that a similar expression for the mild-slope equation given in (26) can be obtained from (29) by discarding the second-order terms:

$$\frac{d^2 \zeta}{dx^2} + P_1 h' \frac{d\zeta}{dx} + k^2 \zeta = 0. \quad (31)$$

The transformation of the complementary mild-slope equation is a little more involved. The relation between ζ and ψ_0 can be found from (7) as $i\omega\zeta = d\psi_0/dx$. Substituting this relation into (24) gives

$$\psi_0 = -\frac{i\omega}{k^2 a + b h'' + (b_h - c) h'^2} \frac{d}{dx} (a\zeta). \quad (32)$$

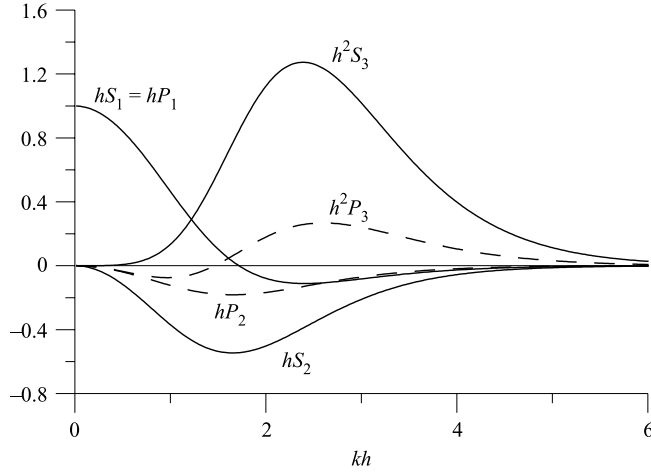


FIGURE 1. Coefficients of complementary and modified mild-slope equations.

Then, the relation $i\omega\zeta = d\psi_0/dx$ gives

$$\frac{d}{dx} \left\{ \frac{1}{k^2a + bh'' + (b_h - c)h'^2} \frac{d}{dx}(a\zeta) \right\} + \zeta = 0, \quad (33)$$

which can be given in a Sturm–Louville type equation as

$$\frac{d}{dx} \left\{ \frac{a^2}{k^2a + bh'' + (b_h - c)h'^2} \frac{d\zeta}{dx} \right\} + a \left\{ 1 + \frac{d}{dx} \left(\frac{2bh'}{k^2a + bh'' + (b_h - c)h'^2} \right) \right\} \zeta = 0. \quad (34)$$

Equation (34) is obviously different from the modified mild-slope equation given in (28). It contains higher-order terms than the modified mild-slope equation, which has the second-order terms $h'^2(x)$ and $h''(x)$ as the highest order. For a fair comparison, (34) is expanded in terms of the bottom slope and curvature up to the second order:

$$\frac{d^2\zeta}{dx^2} + S_1h' \frac{d\zeta}{dx} + (k^2 + S_2h'' + S_3h'^2)\zeta = 0, \quad (35)$$

where

$$S_1(h) = \frac{a_h}{a} - \frac{2k_h}{k}, \quad S_2(h) = \frac{3b}{a}, \quad S_3(h) = \frac{3b_h - c}{a} - \frac{2k_h a_h}{ka} - \frac{a_h^2}{a^2}. \quad (36)$$

Comparing these coefficients with those of the modified mild-slope equation, given by (27) and (30), we can find the following relations for the first two coefficients:

$$S_1 = P_1, \quad S_2 = 3P_2. \quad (37)$$

The remaining coefficients $S_3(h)$ and $P_3(h)$ do not have such relations and are different from each other. All of these coefficients are plotted and compared in figure 1. It can be seen that the terms involved in the second-order terms vanish at the shallow water ($kh \approx 0$) or deep water ($kh = \infty$) limit. At the intermediate depth, where these terms are significant, the difference between the complementary and modified mild-slope equations also becomes significant.

Equations (35) and (37) and figure 1 show that if we take terms up to first order, the complementary mild-slope equation reduces to Berkhoff's mild-slope equation.

However, the second-order terms of the complementary mild-slope equation are different from those of the modified mild-slope equation. The numerical example in §5 shows that the complementary mild-slope equation provides more accurate results. This implies that the second-order terms in the modified mild-slope equation are not necessarily the true second-order correction to Berkhoff's original mild-slope equation. This is presumably because the velocity field assumed in the modified mild-slope equation does not satisfy the bottom boundary condition.

3.2. Conservation laws

Massel (1993) has shown that both the modified mild-slope equation (25) and the mild-slope equation (26) satisfy the following conservation law:

$$\frac{d}{dx} \operatorname{Im} \left[u_0 \zeta^* \frac{d\zeta}{dx} \right] = 0 \quad \text{or} \quad \frac{d}{dx} \operatorname{Im} \left[C C_g \zeta^* \frac{d\zeta}{dx} \right] = 0. \quad (38)$$

A similar conservation law for the complementary mild-slope equation can be derived following the procedure described in Massel (1993) to derive (38). The conservation law is given by

$$\left. \begin{aligned} \frac{d}{dx} \operatorname{Im} \left[\frac{a^2}{k^2 a + b h'' + (b_h - c) h'^2} \zeta^* \frac{d\zeta}{dx} \right] &= 0, \\ \text{or} \\ \frac{d}{dx} \operatorname{Im} \left[\frac{C C_g}{1 - (C^4/g C C_g) \{ b h'' + (b_h - c) h'^2 \}} \zeta^* \frac{d\zeta}{dx} \right] &= 0. \end{aligned} \right\} \quad (39)$$

Equation (39) reduces to (38) when the second-order terms are ignored or when the water depth is uniform.

A relation between the transmission and reflection coefficient can be derived from the conservation law given by (39). Assuming the water depth at far up and downstream are uniform, say $h(-\infty) = h^-$ and $h(\infty) = h^+$, the wave elevation $\zeta(x)$ at up and downstream can be given by

$$\left. \begin{aligned} \zeta &= A(e^{ik^-x} + R e^{-ik^-x}) \quad (x \rightarrow -\infty), \\ \zeta &= AT e^{ik^+x} \quad (x \rightarrow \infty). \end{aligned} \right\} \quad (40)$$

where k^- and k^+ denote the wavenumber at far up and far downstream.

Substituting these expressions into (39), we obtain

$$(C_g)_{h=h^-} (1 - |R|^2) = (C_g)_{h=h^+} |T|^2, \quad (41)$$

which also applies to the full linear theory and other potential-based mild-slope equations (see Kreisel 1949; Massel 1993).

4. Numerical method for two-dimensional diffraction problem

In two dimensions, the complementary mild-slope equation is given as an ordinary differential equation in the domain $-\infty < x < \infty$. Before we present the finite-element method to solve the equation numerically in §4.2, we first derive the radiation condition to confine the computational domain to the finite interval where the bottom varies.

4.1. Radiation condition

We assume that $h(x)$ is continuous in the whole x -axis and varies only in the interval $0 < x < L$, where $h(x)$ is smooth. Outside the variable region, the water depth is

uniform, i.e.

$$\left. \begin{aligned} h(x) &= h^- \quad (x < 0), \\ h(x) &= h^+ \quad (x > L). \end{aligned} \right\} \quad (42)$$

If we denote the wavenumbers for the constant depths as k^- and k^+ , respectively, the asymptotic waves, i.e. the leading terms, in both sides of the interval of varying depth can be expressed in terms of the incoming, the reflected and the transmitted waves as

$$\psi_0(x) \equiv \psi_0^-(x) = \frac{\omega A}{k^-} (e^{ik^-x} - R e^{-ik^-x}) \quad (x < 0), \quad (43)$$

$$\psi_0(x) \equiv \psi_0^+(x) = \frac{\omega A}{k^+} T e^{ik^+x} \quad (x > L), \quad (44)$$

where A is the amplitude of incoming wave and R and T denote the complex reflection and transmission coefficients. In the following, we will restrict the domain of the function $\psi_0(x)$ in the interval $0 < x < L$ and refer to $\psi_0^-(x)$ and $\psi_0^+(x)$ as the solutions in the outer domains at $x < 0$ and $x > L$, respectively.

At $x=0$ and L , where there could be discontinuity in the bottom slope, ψ_0 and $a\psi_0' + bh'\psi_0$ should be continuous for (23) to be valid. In the first term of (23), the derivative should be understood in a generalized (weak) derivative, not in a classical, sense. Then, we have the following jump condition at these endpoints:

$$\psi_0 = \psi_0^-, \quad a^- \frac{d\psi_0}{dx} + b^- h'(+0)\psi_0 = a^- \frac{d\psi_0^-}{dx} \quad \text{at } x = 0, \quad (45)$$

$$\psi_0 = \psi_0^+, \quad a^+ \frac{d\psi_0}{dx} + b^+ h'(L-0)\psi_0 = a^+ \frac{d\psi_0^+}{dx} \quad \text{at } x = L, \quad (46)$$

where $a^\pm \equiv a(h^\pm)$ and $b^\pm \equiv b(h^\pm)$. By the use of (43) and (44), the end conditions, (45) and (46), result in the following radiation conditions for ψ_0 :

$$\frac{d\psi_0}{dx} + \left\{ ik^- + \frac{b^- h'(+0)}{a^-} \right\} \psi_0 = \frac{2iA}{\omega} \quad \text{at } x = 0, \quad (47)$$

$$\frac{d\psi_0}{dx} - \left\{ ik^+ - \frac{b^+ h'(L-0)}{a^+} \right\} \psi_0 = 0 \quad \text{at } x = L. \quad (48)$$

4.2. Numerical implementation

As a numerical procedure to solve the complementary mild-slope equation, we use the finite-element method. The computational domain $0 < x < L$ is divided by $N_x - 1$ segments of equal length $\Delta x = L/(N_x - 1)$. We use piecewise linear shape functions, $\{N_i(x), i = 1, 2, \dots, N_x\}$, as the bases of the trial and test functions. The shape function $N_i(x)$ has a value of one at the i th nodal point, $x_i = (i - 1)\Delta x$, and zero at the other nodal points. In the intervals, the shape function is interpolated linearly. See finite-element textbooks (i.e. Becker, Carey & Oden 1981) for the explicit form of the shape functions. Integrating (23) after multiplying by $N_i(x)$ on both sides, we obtain the weak form of (23) as

$$\int \left\{ \frac{dN_i}{dx} \left(a \frac{d\psi_0}{dx} + bh'\psi_0 \right) + bh'N_i \frac{d\psi_0}{dx} + (-k^2 a + h'^2 c) N_i \psi_0 \right\} dx - ik^- a(h^-) N_i(0) \psi_0(0) - ik^+ a(h^+) N_i(L) \psi_0(L) = \frac{2iAa(h^-) N_i(0)}{\omega}, \quad (49)$$

where integration by parts is made for the first term in (23) and the radiation conditions, (47) and (48), are embedded during the integration by parts.

We also approximate $\psi_0(x)$ by using the same shape functions as

$$\psi_0(x) = \sum_{j=1}^{N_x} \phi_j N_j(x) \quad (50)$$

in the interval $0 < x < L$. Then the weak form in (49) can be reduced to the following algebraic equations:

$$\sum_{j=1}^{N_x} \left[\int \{aN'_i N'_j + bh'(N'_i N_j + N_i N'_j) + (-k^2 a + h'^2 c)N_i N_j\} dx - ik^- a(h^-)N_i(0)N_j(0) - ik^+ a(h^+)N_i(L)N_j(L) \right] \phi_j = \frac{2iAa(h^-)}{\omega} N_i(0) \quad (51)$$

for $i = 1, \dots, N_x$. Once the algebraic equations (51) are solved and the nodal values of the stream function, ϕ_i , are obtained, the reflection and transmission coefficients can be obtained from (43) and (44) and the continuity of the streamfunction at $x = 0$ and L as

$$R = \frac{k^-}{\omega A} \phi_1 - 1, \quad T = \frac{k^+ e^{-ik^+ L}}{\omega A} \phi_{N_x}. \quad (52)$$

5. Numerical results

To test the accuracy and valid range of the complementary mild-slope equation, numerical computations are made for the wave diffraction over three different types of sea bottom. The results are compared to the numerical solution of the full linear theory. Comparisons are also made with the mild-slope and modified mild-slope equations. In the case of the modified mild-slope equation, which was derived by Chamberlain & Porter (1995), the correct radiation condition that satisfies the conservation of mass, proposed by Porter & Staziker (1995), has been used. The numerical results for the full linear theory are obtained by use of the localized finite-element method (Bai & Yeung 1974). The following three examples are taken from Booij (1983) and Porter & Staziker (1995), where the examples were used to test the accuracy of the potential-based mild-slope equations.

5.1. Booij's ramp

As the first example, the linear ramp studied by Booij (1983) is tested. The bathymetry of the ramp is given by

$$h(x) = h_- - \frac{h_+ - h_-}{L} x \quad (0 < x < L). \quad (53)$$

Computations are made by changing the value of L for the condition

$$\frac{h_+}{h_-} = \frac{1}{3}, \quad \frac{\omega^2 h_-}{g} = 0.6. \quad (54)$$

In figure 2, the reflection coefficient $|R|$ is compared with those of the mild-slope equation (Booij 1983), modified mild-slope equation (Chamberlain & Porter 1995; Porter & Staziker 1995) and full linear theory using the localized finite-element method (Bai & Yeung 1974). The present results show better agreement with the

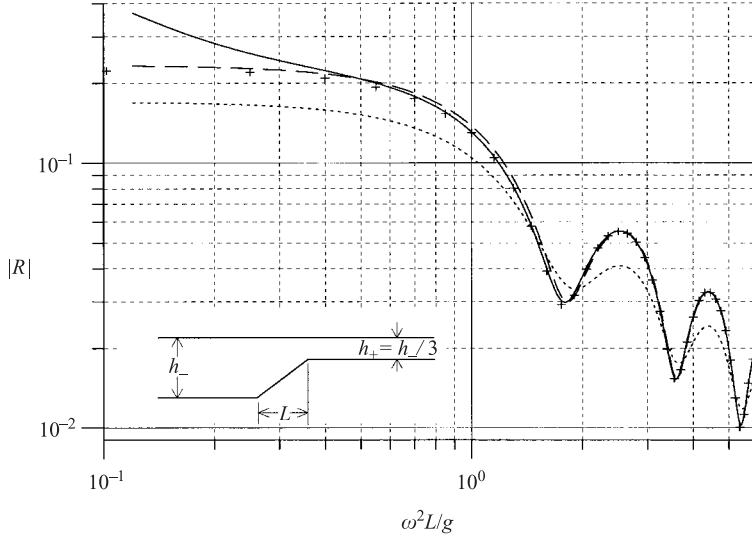


FIGURE 2. Comparison of computed reflection coefficients for Booiij's ramp. +, exact linear theory; ..., mild-slope equation; ---, modified mild-slope equation (Porter & Staziker 1995); —, complementary mild-slope equation.

exact solution than the other mild-slope equations when $\omega^2 L/g$ is greater than 0.6 or the bottom slope is less than 1. When $\omega^2 L/g$ is greater than 0.7, the present result is indistinguishable from the exact solution.

5.2. Parabolic mound

As the second example, wave transmission over a parabolic mound is studied. The shape of the parabolic mound is given by

$$h(x) = h_0 \left\{ 2 \left(\frac{x}{L} \right)^2 - 2 \left(\frac{x}{L} \right) + 1 \right\} \quad (0 < x < L). \quad (55)$$

Porter & Staziker (1995) used the same mound to apply their extended mild-slope equations. Figure 3 shows the comparison of the reflection coefficients calculated by four different methods. The complementary mild-slope equation results agree quite well with the full linear theory when $\omega^2 L/g$ is greater than 2, whereas the original mild-slope provides poor results in the overall range of the mound length. The modified mild-slope equation shows a great improvement, but still with a fair amount of discrepancy. From (55), the maximum slope of the bathymetry is given by $2h_0/L$. As in Booiij's ramp case, the present complementary mild-slope equation model provides accurate results for a bottom slope of less than 1.

5.3. Sinusoidal bed

As the final example, the Bragg scattering over a sinusoidal bed is investigated. The water depth is uniform outside the sinusoidal bed that lies in the region $0 < x < L$, where the variable topography is given by

$$h(x) = h_0 - \delta(x), \quad \delta(x) = d \sin \frac{2\pi}{l} x \quad (0 < x < L), \quad (56)$$

where $l = L/n$ and h_0 is the water depth in the outer region ($h_- = h_+ = h_0$). The

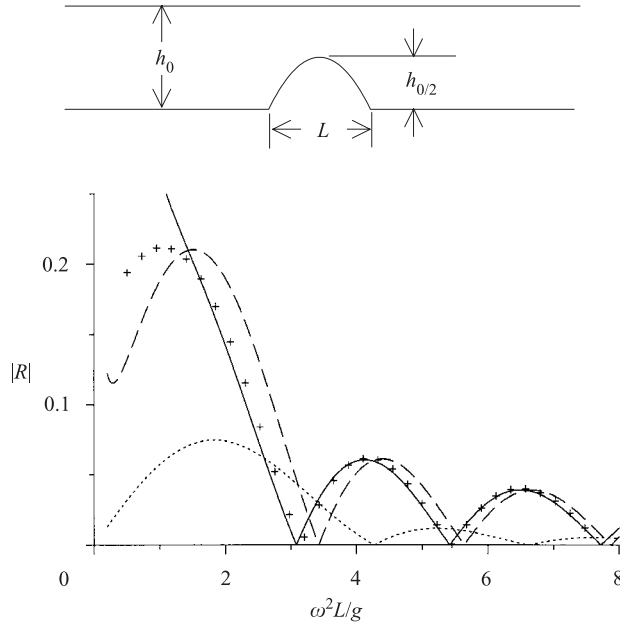


FIGURE 3. Comparison of computed reflection coefficients for parabolic mound ($\omega^2 h_0/g = 1$). +, exact linear theory; \dots , mild-slope equation; $---$, modified mild-slope equation (Porter & Staziker 1995); $—$, complementary mild-slope equation.

bedform consists of a sequence of n sinusoidal ripples about the mean depth $z = -h_0$. When $2l/\lambda = 1$, where λ is the wavelength of the incoming wave, significant reflection occurs owing to the resonant interaction between incoming wave and seabed (see, e.g. Davies & Heathershaw 1984; Mei 1985).

In figure 4, the computed reflection coefficients for a sinusoidal bed with $n = 4$ and $l/h_0 = 6.4$ are shown. Four different amplitudes of the sinusoidal ripple, $d/h_0 = 0.08, 0.16, 0.32$ and 0.64 , are considered in the computation. Again, comparisons are made with the results of the mild-slope equation, extended mild-slope equation and the finite-element solution of the full potential theory. In the overall range of the incoming wavelength, λ , and the ripple amplitude, d , the present results fit accurately to the finite-element results of the full linear theory. The Bragg scattering at $2l/\lambda = 1$ is most accurately predicted by the complementary mild-slope equation than by the other potential-based mild-slope equations. The modified mild-slope equation shows better agreement than the mild-slope equation.

At the small ripple amplitude, $d/h_0 = 0.08$, all three mild-slope equations agree well with the full linear theory. Minor discrepancy was found around $2l/\lambda = 2$ where the potential-based mild-slope equations show slightly higher reflection than the full linear theory and the complementary mild-slope equation. The discrepancy around $2l/\lambda = 2$ grows as the ripple amplitude increases. Other than that area, the potential-based mild-slope equations still agree well with the full linear theory for the ripple amplitudes up to $d/h_0 = 0.16$. When $d/h_0 = 0.32$ the mild-slope equation deviates not only from the full linear theory and the complementary mild-slope equation, but also from the modified mild-slope equation over the whole wavelength range investigated. The modified mild-slope equation shows better agreement yet. The discrepancy between the two potential-based mild-slope equations decreases when the ripple amplitude is

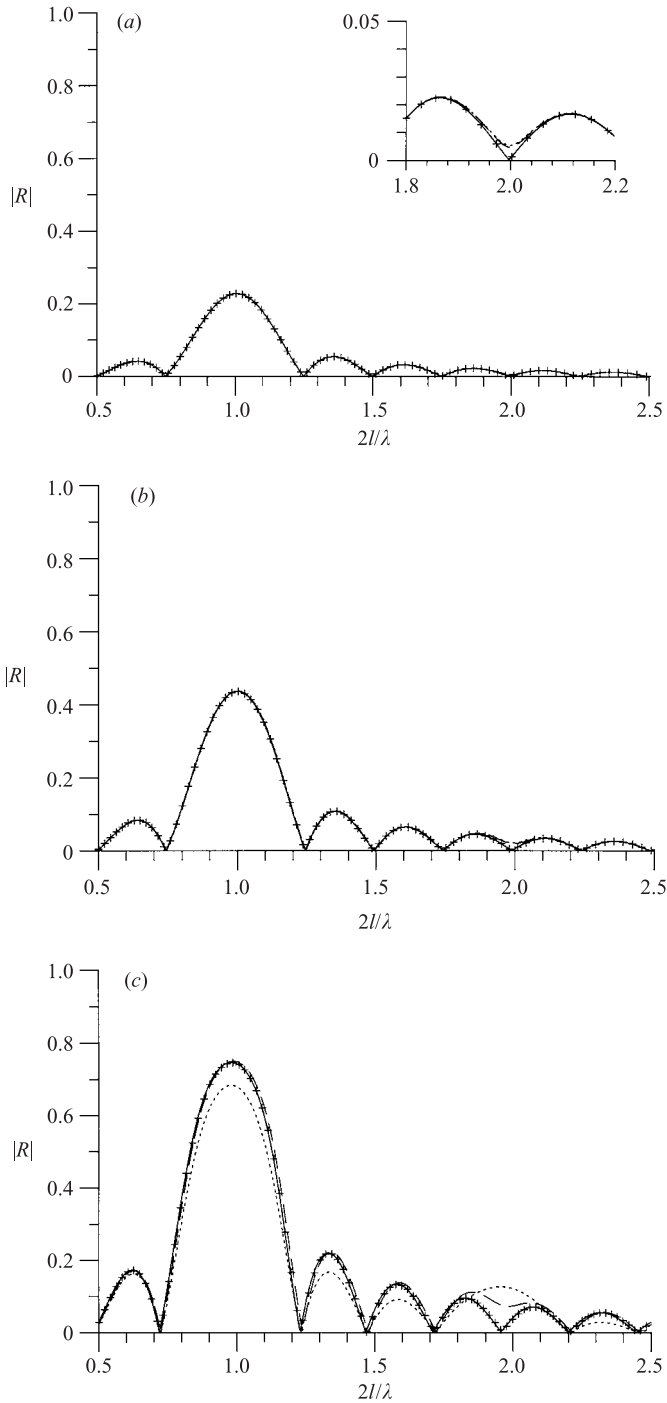
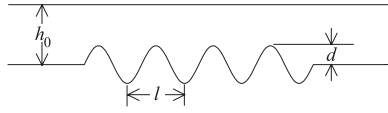


FIGURE 4. For caption see next page.

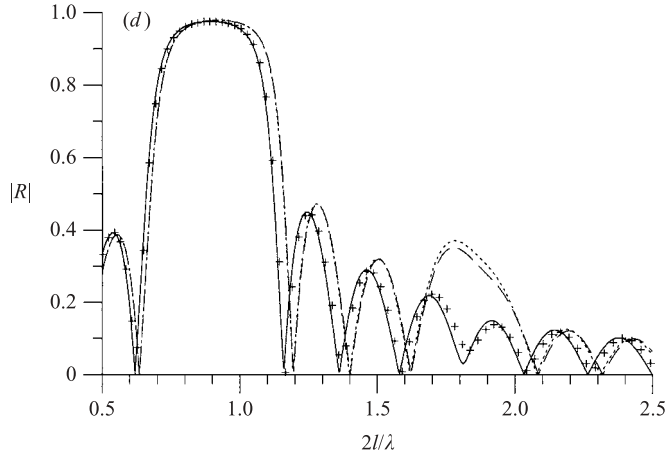


FIGURE 4. Comparison of computed reflection coefficients for ripple bed. +, exact linear theory; ..., mild-slope equation; ---, modified mild-slope equation; —, complementary mild-slope equation. (a) $d/h_0 = 0.08$; (b) 0.16; (c) $d/h_0 = 0.32$; (d) 0.64.

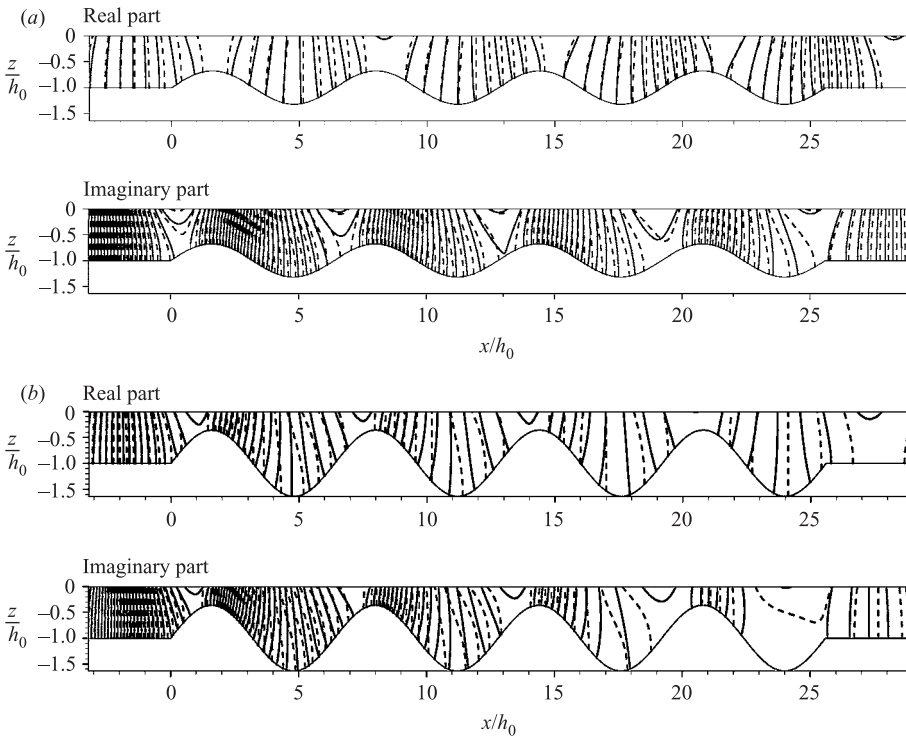


FIGURE 5. Equipotential lines computed for ripple beds with $n = 4$, $l/h_0 = 6.4$ and $2l/\lambda = 1$. Increment of velocity potential value between each equipotential line is $0.2\sqrt{gh}A$. —, exact linear theory; ---, modified mild-slope equation. (a) $d/h_0 = 0.32$; (b) $d/h_0 = 0.64$.

raised to $d/h_0 = 0.64$, where both equations show significant discrepancy from the full linear theory. The complementary mild-slope equation still shows good agreement with the full linear theory at this significantly high ripple amplitude.

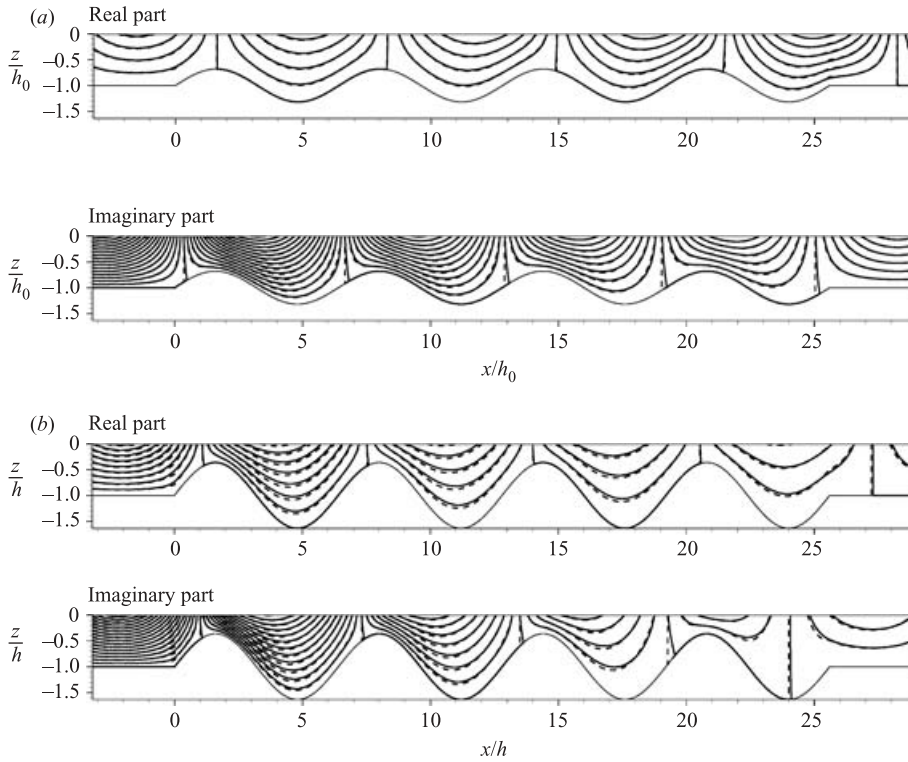


FIGURE 6. Streamlines computed for ripple beds with $n=4$, $l/h_0=6.4$ and $2l/\lambda=1$. Increment of streamfunction value between each streamline is $0.1\sqrt{gh}A$. —, exact linear theory; ---, complementary mild-slope equation. (a) $d/h_0=0.32$; (b) 0.64.

Note that the potential-based mild-slope equations consistently overestimate the reflection coefficient near $2l/\lambda=2$ over the whole ripple amplitude range. Presumably, this is because of the excessive Bragg scattering due to the inaccurate or missing second-order terms in the potential-based mild-slope equations that were discussed in §3.1. The complementary mild-slope equation and the full linear theory show some indication of a weak Bragg scattering near $2l/\lambda=2$ only when the ripple amplitude is significantly high, i.e. $d/h_0=0.64$ as shown in figure 4(d).

In the numerical results so far, only the reflection coefficient has been compared. A more detailed comparison of the flow pattern in the fluid domain is made in figures 5 and 6. The equi-potential lines and streamlines computed from the full linear theory are compared with that from the modified mild-slope equation and the complementary mild-slope equations, respectively. The compared results are for $2l/\lambda=1$, where the reflection coefficient by both the modified and complementary mild-slope equations shows good agreement with the full linear theory. The equi-potential lines by the modified mild-slope equation show a discrepancy with that by the full linear theory, especially near the bottom. The streamlines by the complementary mild-slope equation show much better agreement for both cases of $d/h_0=0.32$ and 0.64, which was anticipated because the complementary mild-slope equation has been derived with the velocity fields that satisfies the boundary condition at the bottom exactly, whereas the velocity fields of the modified mild-slope equation does not.

6. Conclusions

A new type of mild-slope equation, the complementary mild-slope equation, is derived from Hamilton's principle given in terms of streamfunction theory. The new equation shows better performance than the mild-slope equations derived from potential theory. The complementary mild-slope equation provides accurate results for the bottom slope up to 1. The better performance of the present model compared to the potential-based models is presumably due to the exact satisfaction of the bottom boundary condition by the eigenfunction in the streamfunction theory. The new model performed especially well at the sinusoidal beds and bottom mounds. As a result, the complementary mild-slope equation would be an efficient tool to predict the wave diffraction over a steep bathymetry such as the coastal area in the Hawaiian Islands where there are sand bars and reefs on the steep bathymetry. The numerical implementation of the two-dimensional refraction–diffraction model is straightforward and will be pursued in the near future.

K. J. B. was supported by the Korea Research Foundation Grant (KRF-2002-005-D00030).

REFERENCES

- ATHANASSOULIS, G. A. & BELIBASSAKIS, K. A. 1999 A consistent coupled-mode theory for the propagation of small-amplitude water waves over variable bathymetry regions. *J. Fluid Mech.* **389**, 275–301.
- BAI, K. J. 1977 Sway added-mass of cylinders in a canal using dual-extremum principles. *J. Ship Res.* **21**, 193–199.
- BAI, K. J. & YEUNG, R. W. 1974 Numerical solutions of free surface flow problem. *Proc. 10th Symp. Naval Hydrodyn. Office of Naval Research, Cambridge, MA*, pp. 609–641.
- BECKER, E. B., CAREY, G. F. & ODEN, J. T. 1981 *Finite Elements: Volume I. An Introduction*. Prentice-Hall.
- BERKHOFF, J. C. W. 1973 Computation of combined refraction-diffraction. *Proc. 13th Intl Conf. on Coastal Engng, July 1972, Vancouver, Canada*, pp. 471–490. ASCE.
- BOOIJ, N. 1983 A note on the accuracy of the mild-slope equation. *Coastal Engng* **7**, 191–203.
- CHAMBERLAIN, P. G. & PORTER, D. 1995 The modified mild-slope equation. *J. Fluid Mech.* **291**, 393–407.
- CHANDRASEKERA, C. N. & CHEUNG, K. F. 2001 Linear refraction–diffraction model for steep bathymetry. *J. Waterway, Port, Coastal Ocean Engng, ASCE*, **127**, 161–171.
- DAVIES, A. G. & HEATHERSHAW, A. D. 1984 Surface-wave propagation over sinusoidally varying topography. *J. Fluid Mech.* **389**, 275–301.
- KIM, J. W., BAI, K. J., ERTEKIN, R. C. & WEBSTER, W. C. 2001 A derivation of Green–Naghdi equation for irrotational flows. *J. Engng Maths*, **40**, 17–34.
- KIRBY, J. T. 1986 A general wave equation for waves over tipped beds. *J. Fluid Mech.* **162**, 171–186.
- KREISEL, H. 1949 Surface waves. *Q. Appl. Maths* **7**, 21–44.
- MASSEL, S. R. 1993 Extended reflection-diffraction equation for surface waves. *Coastal Engng*, **19**, 97–126.
- MASSEL, S. R. 1993 Extended reflection-diffraction equation for surface waves. *Coastal Engng*, **19**, 97–126.
- MEI, C. C. 1985 Resonant reflection of surface water waves by periodic sandbars. *J. Fluid Mech.* **152**, 315–335.
- MILES, J. W. & CHAMBERLAIN, P. G. 1999 Topological scattering of gravity waves. *J. Fluid Mech.* **361**, 175–188.
- PORTER, D. & STAZIKER, D. J. 1995 Extensions of the mild-slope equation. *J. Fluid Mech.* **300**, 367–382.